JACS
JOURNAL OF THE AMERICAN CHEMICAL SOCIETY

Communication

pubs.acs.org/JACS

Defining Noncovalent Ubiquitin Homodimer Interfacial Interactions through Comparisons with Covalently Linked Diubiquitin

Nicole D. Wagner and David H. Russell*

Department of Chemistry, Texas A&M University, College Station, Texas 77843, United States

Supporting Information

ABSTRACT: Covalently linked diubiquitin (diUbq) is known to adopt specific interfacial interactions owing to steric hindrance induced by the covalent tether. K48-linked diUbq preferentially forms hydrophobic interfacial interactions between the two I44 faces under physiological conditions, whereas K63-linked diUbq preferentially forms electrostatic interfacial interactions. Here, we show using collision-induced unfolding ion mobility-mass spectrometry that the recently reported noncovalent dimer of ubiquitin exhibits structural preferences and interfacial interactions that are most similar to that of K48-linked diUbq.

Ubiquitin (Ubq), a small regulatory protein that is conserved in all eukaryotic cells, functions as a tag for many bioactivities as regulated by its oligomeric state. These bioactive oligomers are formed via an isopeptide bond between the C-terminal carboxyl group of an Ubq subunit and the amino group at either the N-terminus or one of the seven lysine side chains of another Ubq subunit. Ubq bioactivities are encoded by distinct quaternary structures dependent upon the linkage site(s), chain length, branching, and specific noncovalent interactions.[1] Recent investigations have shown that Ubq also forms a noncovalent homodimer (ncUbq) in solution.[2] Tang et al. reported nuclear magnetic resonance (NMR) data that they interpreted as evidence that ncUbq populates an ensemble of conformers where residues surrounding the I44 hydrophobic patch (L8, I44, V70) of each subunit form the dimer interface.[2a] Prag et al. reported a crystal structure of the noncovalent tetramer (teUbq) exhibiting purely electrostatic interfaces.[3] Such differences may arise owing to preferences for "specific interfaces" to remain "dry", whereas "crystal packing interfaces" tend to be "wet".[4] On the basis of cryo-ion mobility-mass spectrometry (cryo-IM-MS) experiments, Servage et al. suggested that water mediates formation and retention of ncUbq ions through formation of intermolecular water-bridges, and that the dimer disassociates to form monomers upon complete evaporation of the water.[2b] Here, we report collision-induced unfolding (CIU) fingerprints that provide additional evidence that ncUbq exhibits similar interfacial interactions and structural stability to diubiquitin (diUbq) covalently linked through K48.

Two covalently linked diUbq were chosen for this study because they each exhibit distinctly different conformations owing to very different interfacial interactions: K48-linked diUbq and K63-linked diUbq. Figure 1 shows representative structures of K48-linked diUbq "closed" and "open" conformers and an "open" conformer of K63-linked diUbq. The two subunits of both diUbq retain much of the native monomeric structure despite the isopeptide linkage, including the preservation of the I44 (L8, I44, V70) and I36 (I36, L71, L73) hydrophobic patches.[1e] Under physiological conditions, K48-linked diUbq preferentially adopts "closed" conformations stabilized by hydrophobic interactions between the two I44 patches (Figure 1A).[1b] Increased protonation of the five basic residues in close proximity to the I44 patch (K6, K11, R42, R72, and H68) induces the preference for electrostatic interfacial interactions, i.e., an "open" conformation (Figure 1B).[1b,5] Reports suggest that K48-linked diUbq exists in equilibrium between the two conformer types.[5b,6] K63-linked diUbq is incapable of forming I44/I44, I44/I36, and I36/I36 interactions and adopts an ensemble of conformer types in solution, viz. an "open" conformation as shown in Figure 1C and two conformers forming electrostatic subunit interfaces.[1c,f,7] Other linkage types (K6-, K11-, etc.) are reported to exhibit a variety of dynamic interfacial interactions

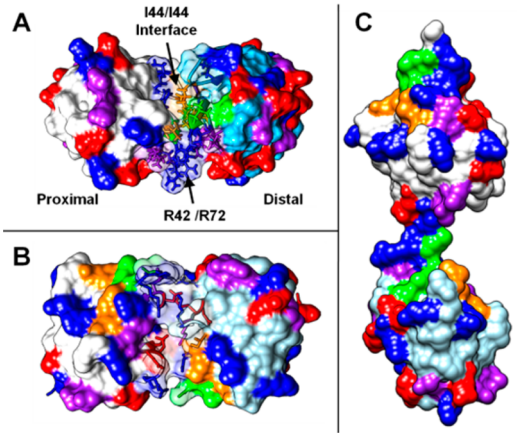

Figure 1. PDB reported structures for (A and B) K48- and (C) K63-linked diUbq, illustrating the different noncovalent interactions responsible for dimer conformational preference. K48-linked diUbq is shown as a "closed" conformation with I44/I44 hydrophobic patch interaction (A, PDB 2PEA) and an "open" conformation with electrostatic interactions (B, PDB 3NS8). K63-linked diUbq is shown with an "open" conformation (C, PDB 2JF5). Note residues are color coded as (blue) basic, (red) acidic, (purple) glutamine and asparagine, (orange) I44 hydrophobic patch, and (green) I36 hydrophobic patch. The calculated CCS values for each are 1780, 1816, and 2086 Å^2 (A–C, respectively).

Received: September 19, 2016
Published: December 14, 2016

DOI: 10.1021/jacs.6b09829
J. Am. Chem. Soc. 2016, 138, 16588–16591

involving either electrostatic interactions or the I36 patch.[8] As such, the hydrophobic I44/I44 interface reported for K48-linked diUbq and the electrostatic interface reported for K63-linked diUbq make each an appropriate model for comparison to ncUbq.

The ESI mass spectrum of Ubq obtained by cryo-IM-MS is dominated by ions corresponding to $[Ubq + 7H]^{7+}$ and $[ncUbq + 14H]^{14+}$ ions;[2b] however, the ESI mass spectrum obtained using ambient conditions contains ions corresponding to $[Ubq + 7H]^{7+}$ and $[Ubq + 8H]^{8+}$ in high abundance, and low abundances of $[ncUbq + 9H]^{9+}$, $[ncUbq + 10H]^{10+}$, and $[ncUbq + 11H]^{11+}$ (see Figure S1 for full mass spectra). The differences in the mass spectra are attributed to the presence of hydrating water molecules in the cryo-IM-MS experiment; note that a large fraction of fully desolvated $[ncUbq + 14H]^{14+}$ ions disassociate to form $[Ubq + 7H]^{7+}$ ions.[2b]

The following discussion will be limited to $[ncUbq + 9H]^{9+}$ and $[ncUbq + 11H]^{11+}$ ions owing to overlap of $[ncUbq + 10H]^{10+}$ and monomeric $[Ubq + 5H]^{5+}$ ions. Figure 2 shows

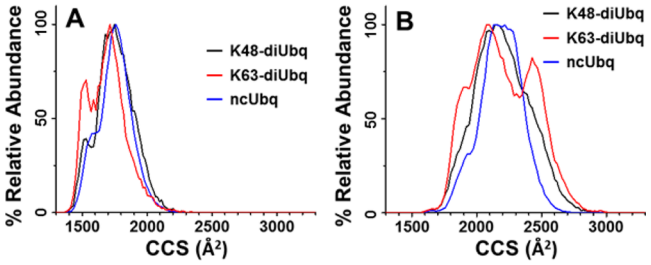

Figure 2. CCS profiles acquired from water and 0.1% formic acid of (A) the 9+ and (B) the 11+ charge states of (black) K48-linked diUbq, (red) K63-linked diUbq, and (blue) ncUbq. All CCS profiles were acquired under ambient conditions and using collision energies of 45 and 55 eV for 9+ and 11+ ions, respectively (the minimum required to maintain ion transmission).

ambient, low internal energy CCS profiles for the 9+ and 11+ charge states of K48- and K63-linked diUbq and ncUbq. Interestingly, under experimental conditions that sample low internal energy ions,[9] each of the ions exhibit similar, conformationally broadened CCS profiles that are practically indistinguishable (see Figure 1 for calculated theoretical CCS values). The 9+ charge state ions of each type suggest at least two conformational populations: a more compact conformer family smaller than all calculated values, i.e., compact (~1500 Å^2), and a more extended conformer family at ~1780 Å^2. These observed CCS values provide strong evidence that the 9+ charge states of each ion exhibit a distribution of conformations similar in size to the reported PDB structures of K48-linked diUbq; note that the calculated CCS values for both conformations of K48-linked diUbq are within the experimental error (±2%) and thus not differentiable using IMS. The 11+ charge state ions of each diUbq demonstrate more conformational heterogeneity and are distinctly larger than the calculated CCS for the K48-linked conformers. The centroid for the CCS profiles are closer to the value calculated for the fully "open" conformation of K63-linked diUbq; however, the detection of the ncUbq 11+ ion suggests that some form of interfacial interactions are preserved. The larger CCS values are attributed to intermediate conformations along the gas-phase unfolding pathway still retaining some form of interfacial interactions. Note that the CCS profiles of K48- and K63-$[diUbq + 14H]^{14+}$ ions suggest that these ions are in an open conformation and that the subunits have significantly unfolded (see Figure S2). These results suggest that the $[ncUbq + 14H]^{14+}$ ion population has disassociated upon complete desolvation similarly to that reported previously.[2b]

Collision-induced unfolding (CIU) and collision-induced dissociation (CID) are increasingly used to investigate conformational changes induced by increasing ion internal energies.[10] CIU combined with IM-MS provides a unique unfolding fingerprint for ions adopting a variety of noncovalent interactions. Here, CIU was used to probe the unfolding fingerprints of the K48- and K63-linked diUbq and ncUbq ions in an effort to elucidate conformational differences/similarities defined by their subunit interfacial interactions. At the collision energies used, covalently linked diUbq does not undergo CID; however, upon destabilization of the ncUbq interface, disassociation to form two intact subunits is observed providing further insight into the relative stability of the ncUbq interface.

Figure 3A,B shows CIU heat maps and the resulting difference plot,[10e] respectively, for the 9+ charge state of K48- and K63-linked diUbq ions. A difference plot is generated by subtraction of two CIU heat maps where features observed of each fingerprint are differentiated as red or blue.[10e] For example in Figure 3B, CCS values observed of K48-linked diUbq are shown in red, whereas those for K63-linked diUbq are shown in blue. The difference plot reveals that K63-$[diUbq + 9H]^{9+}$ ions exhibit a higher abundance of the more compact conformer population than do K48-$[diUbq + 9H]^{9+}$ ions, followed by gradual unfolding up to ~175 eV of collision energy. Upon additional collisional heating, K63-$[diUbq + 9H]^{9+}$ ions undergo a sharp transition from intermediate to extended conformers. Conversely, primarily gradual unfolding is observed for K48-$[diUbq + 9H]^{9+}$ ions, and the collision energy required to populate the most extended conformers of K48-$[diUbq + 9H]^{9+}$ ions is greater than that required to form extended conformers of K63-$[diUbq + 9H]^{9+}$ ions.

Figure 3C,D shows CIU heat maps and difference plot, respectively, for the 11+ charge state of K48- and K63-linked diUbq ions. The CIU heat map for K63-$[diUbq + 11H]^{11+}$ ions reveal that a portion of the ions undergo significant unfolding (to ~2500 Å^2) even at the lowest collision energy; whereas, ~200 eV of collisional energy is required for K48-$[diUbq + 11H]^{11+}$ ions to populate an intermediate conformer with a similar CCS. Furthermore, the collisional activation of K48-$[diUbq + 11H]^{11+}$ ions does not result in distinct unfolding intermediates and produces more compact extended conformers than those observed of K63-$[diUbq + 11H]^{11+}$ ions. Overall, we find that K48- and K63-linked diUbq each exhibit unique unfolding fingerprints, attributable to different tertiary structures and intramolecular stabilization.

Figure 3E,G shows the CIU heat maps for the 9+ and 11+ charge states of ncUbq. The unfolding patterns of the ncUbq ions are visually most similar to those of K48-linked diUbq ions with the same charge state. This observation is further supported by the difference plots shown in Figure 3F,H. The $[ncUbq + 9H]^{9+}$ ion unfolding pattern tracks closely with that of K48-$[diUbq + 9H]^{9+}$ ions up to ~200 eV of collision energy, where some fraction of the total population of K48-$[diUbq + 9H]^{9+}$ ions remains more compact. The 11+ charge states of ncUbq and K48-linked diUbq are less similar to one another than those of the 9+ ions; specifically, the K48-$[diUbq + 11H]^{11+}$ ion conformational population is more broad, i.e., more heterogeneous, than the $[ncUbq + 11H]^{11+}$ conformer population. Overall, we attribute the similarity between the ncUbq and K48-linked diUbq ion CIU fingerprints to similarities in conformation and noncovalent

DOI: 10.1021/jacs.6b09829
J. Am. Chem. Soc. 2016, 138, 16588−16591

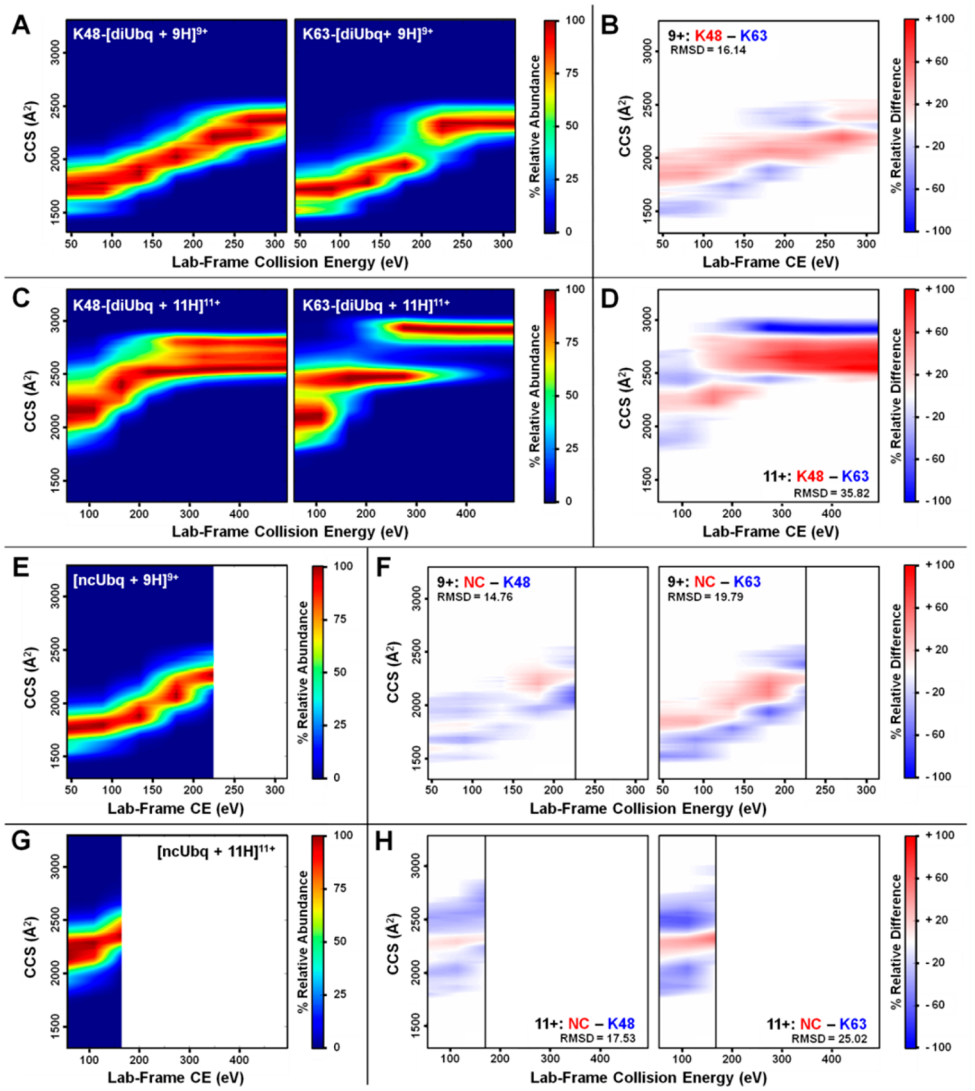

Figure 3. (A and C) CIU heat maps for 9+ and 11+ charge states, respectively, of K48- and K63-linked diUbq ions. (B and D) Difference plots resulting from subtraction of (red) K48- and (blue) K63-linked diUbq CIU profiles for the (B) 9+ and (D) 11+ charge states, respectively. (E and G) CIU heat maps for $[ncUbq + 9H]^{9+}$ and $[ncUbq + 11H]^{11+}$ ions, respectively. (F) Difference plots comparing the CIU unfolding pattern of $[ncUbq + 9H]^{9+}$ to those of (right) K48- and (left) K63-$[diUbq + 9H]^{9+}$ ions. (H) Difference plots comparing the CIU unfolding pattern of $[ncUbq + 11H]^{11+}$ to those of (right) K48- and (left) K63-$[diUbq + 11H]^{11+}$ ions. Note that all collision energies are reported as lab-frame kinetic energy and that each CCS profile is normalized to the most abundant feature.

interactions. The CIU fingerprints for both charge states of K63-linked diUbq differ dramatically from those of the ncUbq ions, further strengthening this assessment. Note that CIU heat maps for K6- and K11-linked diUbq ions[1e] are more similar to K63-linked diUbq than to K48-linked diUbq and ncUbq ions. These comparisons provide further support for our assignment (see Figure S3; note the large change in CCS rather than gradual unfolding).

The CIU heat maps for ncUbq ions are truncated due to collision-induced disassociation (see Figure S4 for a detailed description of the CID of ncUbq ions). Interestingly, both the $[ncUbq + 9H]^{9+}$ and $[ncUbq + 11H]^{11+}$ ions are stable through collision energies that produce intermediate conformers of K48-linked diUbq but disassociate prior to formation of the most extended conformations of K48-linked diUbq. The disassociation of ncUbq ions occurs at collision energies larger than those resulting in extended K63-linked diUbq conformers. This further supports our hypothesis that the noncovalent interactions stabilizing ncUbq are more similar to those of the K48-linked diUbq ions. Furthermore, the disassociation of ncUbq at a collision energy below that required for formation of the most extended conformers of K48-linked diUbq suggests that this final transition corresponds to complete disruption of the K48-linked diUbq noncovalent interface.

Overall, we have shown that the tertiary structures of the closed conformations of K48- and K63-linked diUbq are differentiable using CIU, suggesting that the method is sensitive to differences in protein−protein interfacial interactions. Furthermore, the results of CIU support previously published results suggesting that ncUbq adopts an I44/I44 hydrophobic interface in solution as opposed to primarily electrostatic interactions.[2] Fushman suggested that the prevalence of the K48-linked diUbq hydrophobic interface in solution is pH dependent, i.e., the preference for the I44/I44 interface is dependent upon the protonation state of basic residues in close proximity to the interface.[5b] Due to this pH dependence, control studies were performed for ncUbq and K48- and K63-linked diUbq using buffered solution. The buffered solutions produced 7−9+ charge

DOI: 10.1021/jacs.6b09829
J. Am. Chem. Soc. 2016, 138, 16588−16591

states of each (see Figure S5 for the full MS). When the CIU fingerprints produced from buffered solution were compared to the 9+ ions produced from acidic solution, the difference plots show little deviation (see Figure S6). The most notable difference between the CIU patterns from buffered and acidic solutions correspond to collapsed conformers that are observed at low collision energies from acidic solution (~1500 Å^2). We attribute these more collapsed conformers to an acid-induced, molten globule conformation.[12] Note that 11+ ncUbq and diUbq ions were not observed from buffered solution and as such may be more representative of acid destabilized conformations.

Liu et al. predicted a dissociation constant for ncUbq of 4.4 mM, higher than the concentrations used in this study.[2a] Electrospray ionization (ESI) produces charged nanodroplets that contain the analyte of interest. The effective concentration of the analyte may increase as the droplet size decreases; therefore, in the late stages of droplet evolution, the concentration of Ubq may approach the K_D of ncUbq. Consequently, it is possible that the ncUbq ions presented in this study may not be representative of initial solution-phase conformations, but rather "ESI-induced" dimerization.[13] The cryo-IM-MS experiment has the advantage of monitoring hydrated proteins en route to complete desolvation. Servage et al. report that $[ncUbq + 14H]^{14+}$ ions exhibit a hydration trendline, whereas $[Ubq + 7H]^{7+}$ does not.[2b] The absence of Ubq hydration suggests that nonspecific dimerization of Ubq is preferred either during the ESI process or in solution.

Servage et al. also speculated that the basic residues surrounding the hydrophobic patch serve as hydration sites, resulting in two modes of interfacial stabilization: to promote occlusion of water from the hydrophobic interface and to reduce Coulombic repulsion via water bridging.[2b] A recent report suggests that charged residues serve as recognition sites for both mono- and pUbq by the proteosome prior to forming final hydrophobic interactions.[11] Arginine is one of three residues found with greater than 10% incidence in protein hot spots.[14] The proximity of the R42 and R72 residues from both ubiquitin subunits to the interface of "closed" K48-linked diUbq[1b,5] and the precedence for arginine participation in hot spots suggests that these residues would have a strong impact on the binding strength of the ncUbq subunit interface. An ionic hydrogen bond between a guanidinium ion and a proximal guanidine group would impart significant stabilization to the subunit interface, especially upon desolvation; whereas, if multiple guanidine groups are protonated, then Coulombic repulsion may induce disassociation of the hydrophobic interface. The similarities between the ncUbq and K48-linked diUbq CIU patterns and the effects of pH portend the inclusion of the arginine residues as part of the ncUbq hot spot. In conclusion, CIU provides further evidence for the ncUbq hot spot to include the I44 hydrophobic patch and proximal R42/R72 arginine residues.

■ ASSOCIATED CONTENT

Supporting Information

The Supporting Information is available free of charge on the ACS Publications website at DOI: 10.1021/jacs.6b09829.

Experimental details, mass spectra, the results of CID, and CIU heat maps for alternative linkage types and buffered solution (PDF)

■ AUTHOR INFORMATION

Corresponding Author

*russell@chem.tamu.edu

ORCID

David H. Russell: 0000-0003-0830-3914

Notes

The authors declare no competing financial interest.

■ ACKNOWLEDGMENTS

Molecular graphics were prepared with the UCSF Chimera package. Theoretical CCS values were calculated by Dr. Doyong Kim. This research was supported by U.S. Department of Energy, Division of Chemical Sciences, Basic Energy Science (DE-FG02-04ER15520).

■ REFERENCES

(1) (a) Avram, H. In *The Ubiquitin System*; Peters, J.-M.; Harris, J. R., Finley, D., Eds.; Springer, 1998. (b) Varadan, R.; Walker, O.; Pickart, C.; Fushman, D. *J. Mol. Biol.* **2002**, *324*, 637−647. (c) Varadan, R.; Assfalg, M.; Haririnia, A.; Raasi, S.; Pickart, C.; Fushman, D. *J. Biol. Chem.* **2004**, *279*, 7055−7063. (d) Fushman, D.; Wilkinson, K. D. *F1000 Biol. Rep.* **2011**, *3*, 26. (e) Komander, D.; Rape, M. *Annu. Rev. Biochem.* **2012**, *81*, 203−229. (f) Ye, Y.; Blaser, G.; Horrocks, M. H.; Ruedas-Rama, M. J.; Ibrahim, S.; Zhukov, A. A.; Orte, A.; Klenerman, D.; Jackson, S. E.; Komander, D. *Nature* **2012**, *492*, 266−270.

(2) (a) Liu, Z.; Zhang, W. P.; Xing, Q.; Ren, X.; Liu, M.; Tang, C. *Angew. Chem., Int. Ed.* **2012**, *51*, 469−472. (b) Servage, K. A.; Silveira, J. A.; Fort, K. L.; Clemmer, D. E.; Russell, D. H. *J. Phys. Chem. Lett.* **2015**, *6*, 4947−4951.

(3) Levin-Kravets, O.; Shohat, N.; Prag, G. *Biochemistry* **2015**, *54*, 4704−4710.

(4) Rodier, F.; Bahadur, R. P.; Chakrabarti, P.; Janin, J. *Proteins: Struct., Funct., Genet.* **2005**, *60*, 36−45.

(5) (a) Ryabov, Y.; Fushman, D. *Proteins: Struct., Funct., Genet.* **2006**, *63*, 787−796. (b) Lai, M. Y.; Zhang, D.; Laronde-Leblanc, N.; Fushman, D. *Biochim. Biophys. Acta, Mol. Cell Res.* **2012**, *1823*, 2046−2056.

(6) Hirano, T.; Serve, O.; Yagi-Utsumi, M.; Takemoto, E.; Hiromoto, T.; Satoh, T.; Mizushima, T.; Kato, K. *J. Biol. Chem.* **2011**, *286*, 37496−37502.

(7) (a) Komander, D.; Reyes-Turcu, F.; Licchesi, J. D. F.; Odenwaelder, P.; Wilkinson, K. D.; Barford, D. *EMBO Rep.* **2009**, *10*, 466−473. (b) Liu, Z.; Gong, Z.; Jiang, W. X.; Yang, J.; Zhu, W. K.; Guo, D. C.; Zhang, W. P.; Liu, M. L.; Tang, C. *eLife* **2015**, *4*, DOI: 10.7554/eLife.05767.

(8) (a) Matsumoto, M. L.; Wickliffe, K. E.; Dong, K. C.; Yu, C.; Bosanac, I.; Bustos, D.; Phu, L.; Kirkpatrick, D. S.; Hymowitz, S. G.; Rape, M.; Kelley, R. F.; Dixit, V. M. *Mol. Cell* **2010**, *39*, 477−484. (b) Virdee, S.; Ye, Y.; Nguyen, D. P.; Komander, D.; Chin, J. W. *Nat. Chem. Biol.* **2010**, *6*, 750−757. (c) Bremm, A.; Komander, D. *Trends Biochem. Sci.* **2011**, *36*, 355−363. (d) Wickliffe, K. E.; Williamson, A.; Meyer, H. J.; Kelly, A.; Rape, M. *Trends Cell Biol.* **2011**, *21*, 656−663.

(9) Chen, S. H.; Russell, D. H. *J. Am. Soc. Mass Spectrom.* **2015**, *26*, 1433−1443.

(10) (a) Hopper, J. T. S.; Oldham, N. J. *J. Am. Soc. Mass Spectrom.* **2009**, *20*, 1851−1858. (b) Cubrilovic, D.; Biela, A.; Sielaff, F.; Steinmetzer, T.; Klebe, G.; Zenobi, R. *J. Am. Soc. Mass Spectrom.* **2012**, *23*, 1768−1777. (c) Laganowsky, A.; Reading, E.; Allison, T. M.; Ulmschneider, M. B.; Degiacomi, M. T.; Baldwin, A. J.; Robinson, C. V. *Nature* **2014**, *510*, 172−175. (d) Liu, J.; Konermann, L. *J. Am. Soc. Mass Spectrom.* **2014**, *25*, 595−603. (e) Eschweiler, J. D.; Rabuck-Gibbons, J. N.; Tian, Y.; Ruotolo, B. T. *Anal. Chem.* **2015**, *87*, 11516−11522.

(11) Zhang, Y.; Vuković, L.; Rudack, T.; Han, W.; Schulten, K. *J. Phys. Chem. B* **2016**, *120*, 8137−8146.

(12) Baldwin, R. L.; Rose, G. D. *Curr. Opin. Struct. Biol.* **2013**, *23*, 4−10.

(13) Kebarle, P.; Verkerk, U. H. *Mass Spectrom. Rev.* **2009**, *28*, 898−917.

(14) Bogan, A. A.; Thorn, K. S. *J. Mol. Biol.* **1998**, *280*, 1−9.

DOI: 10.1021/jacs.6b09829
J. Am. Chem. Soc. 2016, 138, 16588−16591